

## ULTRAVIOLET IMAGERY OF NGC 6752: A TEST OF EXTREME HORIZONTAL BRANCH MODELS

WAYNE B. LANDSMAN,<sup>1</sup> ALLEN V. SWEIGART,<sup>2</sup> RALPH C. BOHLIN,<sup>3</sup> SUSAN G. NEFF,<sup>2</sup> ROBERT W. O'CONNELL,<sup>4</sup> MORTON S. ROBERTS,<sup>5</sup>  
 ANDREW M. SMITH,<sup>2</sup> AND THEODORE P. STECHER<sup>2</sup>

Received 1996 July 18; accepted 1996 September 18

### ABSTRACT

We present a 1620 Å image of the nearby globular cluster NGC 6752 obtained with the Ultraviolet Imaging Telescope (UIT) during the Astro-2 mission of the Space Shuttle *Endeavour* in 1995 March. An ultraviolet-visible color-magnitude diagram (CMD) is derived for 216 stars matched with the visible photometry of Buonanno et al. This CMD provides a nearly complete census of the hot horizontal-branch (HB) population with good temperature and luminosity discrimination for comparison with theoretical tracks.

The observed data show good agreement with the theoretical zero-age horizontal branch (ZAHB) of Sweigart for an assumed reddening of  $E(B - V) = 0.05$  and a distance modulus of 13.05. The observed HB luminosity width is in excellent agreement with the theoretical models and supports the single-star scenario for the origin of extreme horizontal branch (EHB) stars. However, only four stars can be identified as post-EHB stars, whereas almost three times this many are expected from the HB number counts. If this effect is not a statistical anomaly, then some noncanonical effect may be decreasing the post-EHB lifetime. The recent noncanonical models of Sweigart, which have helium-enriched envelopes due to mixing along the red giant branch, cannot explain the deficit of post-EHB stars, but might be better able to explain their luminosity distribution.

*Subject headings:* globular clusters: individual (NGC 6752) — stars: horizontal-branch — ultraviolet: stars

### 1. INTRODUCTION

The evolution of extreme horizontal branch (EHB) stars has attracted considerable interest in recent years due to their importance for understanding the hot stellar population in both metal-poor and metal-rich stellar systems (e.g., Caloi 1989; Castellani et al. 1994). According to canonical theory, EHB stars retain only a thin ( $<0.02 M_{\odot}$ ) inert hydrogen envelope due to prior mass loss on the red giant branch (RGB), and spend their core-helium-burning lifetime at high effective temperatures ( $20,000 \text{ K} \leq T_{\text{eff}} \leq 35,000 \text{ K}$ ). Following the exhaustion of their central helium, EHB stars do not return to the asymptotic giant branch (AGB) but instead follow AGB-manqué tracks, spending the rest of their pre-white dwarf lifetime at high temperatures and luminosities. Because of their sustained hot phases, EHB and post-EHB stars are the most promising candidates for producing the ultraviolet excess observed in elliptical galaxies (Greggio & Renzini 1990; Dorman, O'Connell, & Rood 1995; Yi et al. 1995).

Several scenarios have been suggested to explain the origin of EHB stars. In the single-star scenario, EHB stars are produced by extensive mass loss along the RGB, which reduces the envelope mass to the very small values required by canonical EHB models. This scenario predicts that the EHB should appear as a well-defined extension of the blue horizontal branch (BHB) in the color-magnitude diagram (CMD). The principal difficulty with this scenario is the fine tuning of

the mass-loss process needed to produce the narrow range of EHB envelope masses. To avoid this fine-tuning problem, D'Cruz et al. (1996) have suggested that some EHB stars might be "hot He-flashers," i.e., stars which evolve off the RGB to high effective temperatures before igniting helium. Such stars would settle onto a blue hook at the hot end of the HB. Several binary scenarios have also been proposed, involving either Roche lobe overflow along the RGB or the merger of a double helium white dwarf system (see Bailyn 1995 for a review). These scenarios predict a wide range in the EHB mass and therefore a wide range in luminosity.

Theoretical EHB models have not been well tested even in the globular clusters. The main observational difficulty has been the derivation of accurate luminosities and temperatures for a large sample of EHB and post-EHB stars, for comparison with theoretical predictions. In a standard  $(V, B - V)$  CMD, the EHB is observed as a nearly vertical blue tail, and the effect of an increase in temperature is nearly degenerate with that of a decrease in luminosity. Ultraviolet observations can provide the needed temperature discrimination, but, while previous ultraviolet experiments have yielded some intriguing discrepancies with canonical hot HB models (Whitney et al. 1994; Dixon et al. 1996), they have lacked either the sensitivity or the spatial resolution for a clean confrontation with the theory.

The recent noncanonical HB models of Sweigart (1996) provide a further impetus for an observational test of EHB and post-EHB evolution. These models include the dredge-up of helium from the hydrogen shell on the RGB, as possibly suggested by the observed abundance anomalies in globular cluster red giants (e.g., Langer & Hoffman 1995). A star that undergoes such helium mixing will arrive on the HB with an enhanced envelope helium abundance and therefore will lie blueward of its canonical location. In this scenario, the high effective temperatures of EHB stars are due to a high envelope helium abundance, which considerably increases the envelope

<sup>1</sup> Hughes STX Corporation, NASA Goddard Space Flight Center, Laboratory for Astronomy and Solar Physics, Code 681, Greenbelt, MD 20771.

<sup>2</sup> NASA Goddard Space Flight Center, Laboratory for Astronomy and Solar Physics, Code 681, Greenbelt, MD 20771.

<sup>3</sup> Space Telescope Science Institute, 3700 San Martin Drive, Baltimore, MD 21218.

<sup>4</sup> University of Virginia, Department of Astronomy, P.O. Box 3818, Charlottesville, VA 22903.

<sup>5</sup> National Radio Astronomy Observatory, 520 Edgemont Rd., Charlottesville, VA 22903.

TABLE 1  
POST-EHB CANDIDATES IN NGC 6752

Name	SWP	$V$	$B - V$	$m_{162}$	$\log T_{\text{eff}}$	$\log L/L_{\odot}$
B852 <sup>a</sup> .....	55397	15.91	-0.28	11.89	4.49	2.05
B1754 <sup>a</sup> .....	19441	15.99	-0.24	11.82	4.54	2.12
B2004 <sup>a, b</sup> .....	55384	16.42	-0.31	12.11	4.66	2.25
B4380 .....	55548	15.93	-0.14	12.01	4.46	2.00
UIT 1 <sup>c</sup> .....	55383	...	...	11.42	...	...

<sup>a</sup> sdO optical spectrum; Moehler et al. 1996 and S. Moehler (1996, private communication).

<sup>b</sup> Uncertain UIT and *IUE* fluxes due to contamination from the nearby (2".5 distant) hot HB star B1995.

<sup>c</sup> R.A.(2000):  $19^{\text{h}}10^{\text{m}}54^{\text{s}}.01$ , decl.(2000):  $-59^{\circ}59'46''.2$ .

masses. Thus the problem of fine tuning the mass-loss process is avoided.

NGC 6752 is a nearby  $[(m - M)_0 = 13.05]$ , lightly reddened  $[E(B - V) \sim 0.04]$ , intermediate metallicity  $[\text{Fe}/\text{H}] = -1.64$  globular cluster with a blue HB and a large population of EHB stars (Buonanno et al. 1986, hereafter B86). The quoted distance for NGC 6752 is taken from the recent *HST* observations of the white dwarf cooling curve by Renzini et al. (1996, hereafter R96), and thus is independent of any assumptions concerning the HB luminosity. In 1995 March, we imaged NGC 6752 at 1620 Å using the Ultraviolet Imaging Telescope (UIT), which was part of the Astro-2 Space Shuttle payload. The UIT field of view (40') is well matched to the cluster size, and its solar-blind CsI detectors suppress the dominant cool star population and allow hot HB stars to be detected into the center of the cluster. In this Letter, we combine the UIT photometry with the visible photometry of B86 to derive temperatures and luminosities for a large sample of EHB and post-EHB stars for comparison with theoretical predictions.

## 2. OBSERVATIONS

The UIT uses image-intensified film detectors and has a spatial resolution of about 3" (Stecher et al. 1992). NGC 6752 was observed with the B5 filter, which has a central wavelength of 1620 Å and a width of about 225 Å (Stecher et al. 1992). Only the deepest (781 s) image (FUV2619) obtained on 1995 March 8 is used here (Fig. 1 [Pl. L10]). The magnitudes,  $m_{162}$ , given in this Letter are defined as  $-2.5 \times \log f_{\lambda} - 21.1$ , where  $f_{\lambda}$  is the mean flux through the B5 filter. The UV photometry was derived by PSF fitting using an IDL implementation of the DAOPHOT algorithms of Stetson (1987), with the error analysis modified for use with film. The complete UV photometry catalog, along with a discussion of the radial distribution of the hot HB stars, will be reported in a subsequent paper.

The UIT image of NGC 6752 shows five stars significantly brighter than the other 354 detected hot stars. Three of these stars were classified as post-EHB stars by Moehler, Heber, & Rupprecht (1996), while one is interior to the annulus studied by B86, and is designated here as UIT 1. Only one of these stars (B1754) had been previously observed with *IUE*, and so we have obtained short-wavelength (SWP), low-dispersion *IUE* spectra of the other four (Table 1). The *IUE* spectra each show a hot continuum but have insufficient S/N to allow certain identification of any spectral features. The UIT photometry is used to derive  $T_{\text{eff}}$  and  $\log L$  in Table 1, because the *IUE* spectra of three of the post-EHB candidates (B1754, B2004, UIT 1) are contaminated by neighboring hot HB stars.

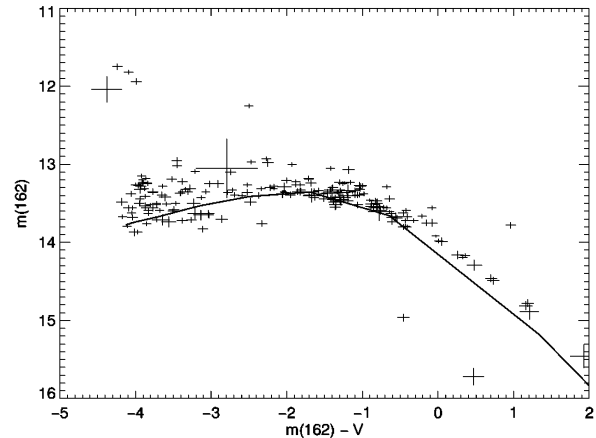


FIG. 2.—Ultraviolet-visible CMD for 216 stars in NGC 6752. The error bars are derived from the ultraviolet photometry, and assume a 0.03 mag uncertainty in the visible photometry. The solid line shows the canonical ZAHB of Sweigart (1996) for  $[\text{Fe}/\text{H}] = -1.5$ , assuming  $(m - M)_0 = 13.05$  and  $E(B - V) = 0.05$ .

The absolute calibration was determined by comparison with the 14 HB stars observed with *IUE* by Cacciari et al. (1995) plus the four new ones reported here. The *IUE* spectra were processed using the NEWSIPS reduction (Nichols & Linsky 1996), but with the absolute calibration corrected to the Bohlin (1996) scale. There is a standard deviation of 0.075 mag between the *IUE* and UIT fluxes, which is about what is expected for the two instruments.

Temperatures are derived from the  $m_{162} - V$  color using the LTE model atmospheres of Kurucz (1993) for  $[\text{Fe}/\text{H}] = -1.5$  and assuming  $E(B - V) = 0.05$ . This reddening value was adopted to yield the best agreement between our  $T_{\text{eff}}$  values and those derived from Balmer line fitting by Moehler et al. (1996), and is close to the value of  $E(B - V) = 0.04$  tabulated by Peterson (1993). There is evidence for an increasing discrepancy between the two methods of determining  $T_{\text{eff}}$  for  $T_{\text{eff}} > 30,000$  K (with Balmer line fitting yielding higher temperatures), perhaps because non-LTE effects are more important at these high temperatures, or perhaps because the  $V$  magnitudes are less reliable for the hottest (and faintest) HB stars.

There is a 97% overlap between the hot ( $B - V < 0.22$ ) stars in the B86 catalog and the stars detected on the UIT image in the same area of the cluster (roughly between 1.5 and 9.5' from the cluster center). Ultraviolet fluxes could not be determined for three HB stars on the UIT image that are too close to the heavily saturated foreground star HD 177999. The spatial resolution of UIT was insufficient to obtain useful photometry for the hot HB stars B1525 and B1532, which are separated by 2".8. Finally, two stars detected on the UIT image could not be matched with any blue stars in B86, and instead appear to be matched with "red stragglers" stars with composite colors. B4840 ( $V = 13.64$ ,  $B - V = 0.87$ ) is likely a composite of a hot HB star and a red giant, while B1370 ( $V = 16.09$ ,  $B - V = 0.33$ ) is likely a composite of a hot HB star and a subgiant. Further observations are needed to determine whether these composite colors indicate a physical association.

## 3. DISCUSSION

Figure 2 shows an ultraviolet-visible CMD for the 216 UIT stars in common with B86 together with the canonical zero-age

## PLATE L10

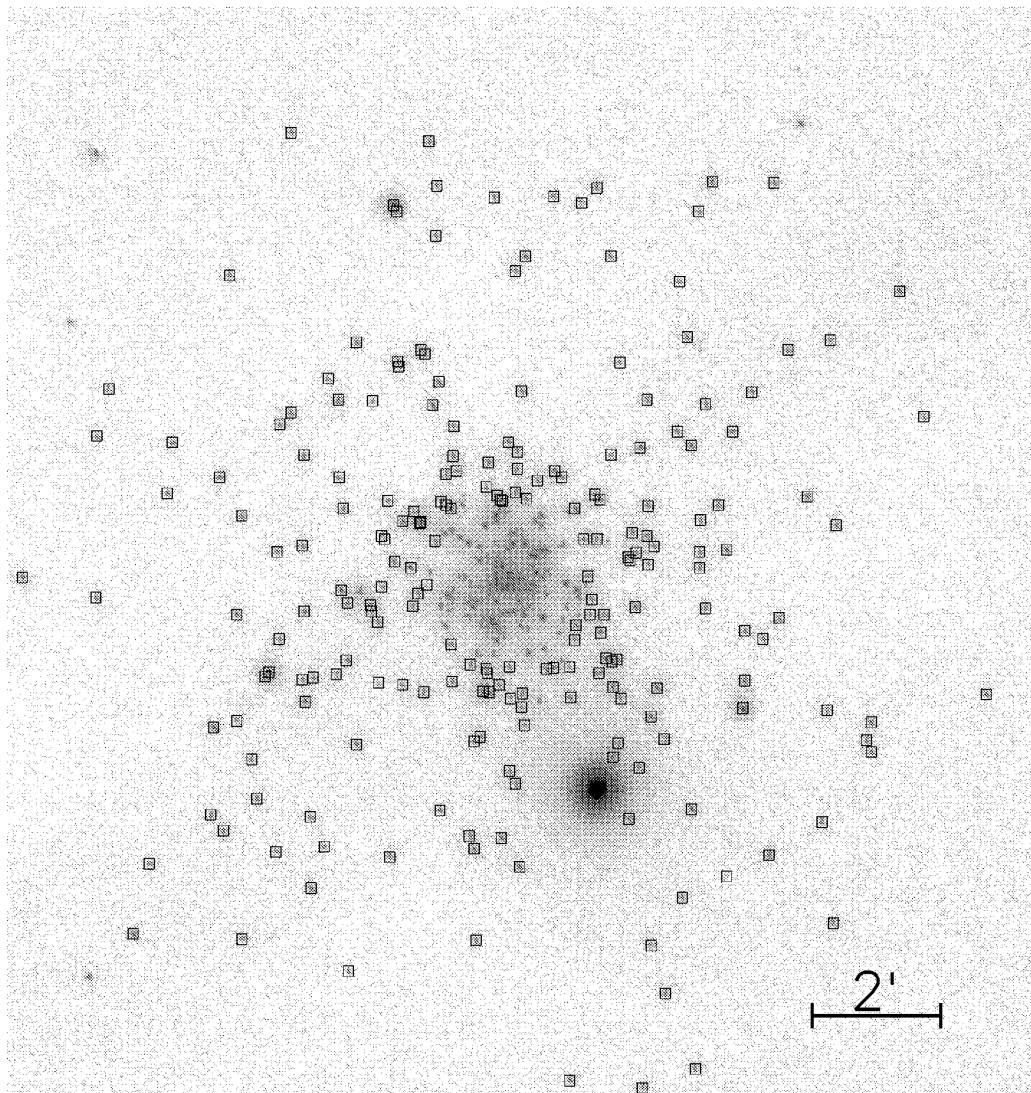


FIG. 1.—UIT 1620 Å image of NGC 6752. North is up and east is to the left. The heavily saturated source 4' southwest of the cluster is the foreground star HD 177999 ( $V = 7.4$ , B9 II–III). The 216 stars used in the CMD are marked with boxes.

LANDSMAN et al. (472, L94)



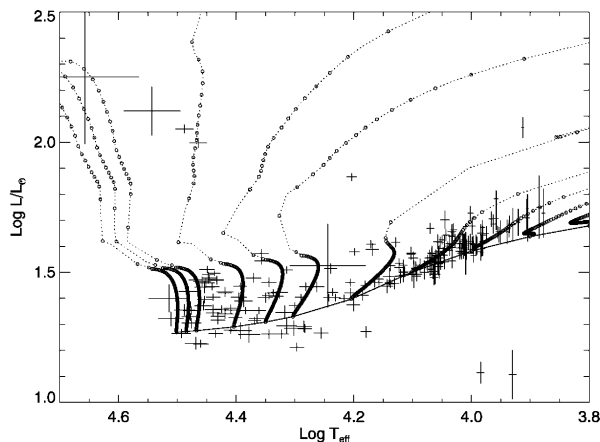


FIG. 3.—UIT data from Fig. 2 are shown transformed to the theoretical plane for  $(m - M)_0 = 13.05$  and  $E(B - V) = 0.05$ . The error bars are derived from the photometric errors propagated into the  $(\log T_{\text{eff}}, \log L)$ -plane. Also shown is the theoretical ZAHB of Sweigart (1996) along with selected evolutionary tracks. The rate of evolution along the tracks is indicated by the small circles, which are separated by a time interval of  $10^6$  yr.

HB (ZAHB) from Sweigart (1996) for a scaled-solar metallicity of  $Z = 5 \times 10^{-4}$  and a main-sequence helium abundance of  $Y = 0.23$ . As noted by B86, the CMD shows a relative deficit of HB stars near  $m_{162} - V = -2.7$  ( $\log T_{\text{eff}} \sim 4.25$ ). The two cool stars (B1624 and B2044) that fall considerably below the ZAHB are probably either nonmembers or extreme blue stragglers. The distribution of hot stars shows excellent agreement with the theoretical ZAHB for the assumed distance and reddening, except that the hottest stars appear to be too faint by  $\sim 0.1$ – $0.2$  mag. This offset could be explained if the core mass in EHB stars was  $\sim 0.01$ – $0.02 M_{\odot}$  smaller than the canonical value. In any case, Figure 2 suggests that the difference in the ZAHB luminosity between the EHB and BHB may be somewhat larger than predicted by canonical models. We note that the hot He-flasher stars discussed by D’Cruz et al. (1996) are predicted to lie up to  $\sim 0.1$  mag below the canonical ZAHB. However, such stars are constrained to a small temperature range around  $\log T_{\text{eff}} \sim 4.5$  ( $m_{162} - V \sim -4$ ), and thus should appear as a blue hook at the hot end of the EHB. No such feature is evident in Figure 2.

Our observational data are plotted in the theoretical plane in Figure 3 together with selected evolutionary tracks. Figure 3 shows that the predicted luminosity width of the HB is in excellent agreement with the observations, with the width increasing from about 0.1 dex near  $\log T_{\text{eff}} = 4.0$  to about 0.25 dex near  $\log T_{\text{eff}} = 4.5$ . The EHB in NGC 6752 thus appears to be an extension of the BHB, as predicted by the single-star scenario for the origin of EHB stars.

We next consider the four post-EHB stars<sup>6</sup> in Figure 3. The evolutionary tracks with ZAHB effective temperatures greater than  $\log T_{\text{eff}} \sim 4.30$  show a long-lived, hot, post-EHB phase. The theoretical lifetime of this post-EHB phase is typically 0.15–0.20 of the EHB lifetime itself. Since the CMD contains 63 stars hotter than  $\log T_{\text{eff}} = 4.30$ , one would therefore expect about 10 post-EHB stars, compared to the four actually found. We have done Monte Carlo simulations to determine the probability of finding only four post-EHB stars. Stars are

<sup>6</sup> The star B2485 with  $\log T_{\text{eff}} \sim 4.2$  and  $\log L \sim 1.8$  in Fig. 3 is a possible fifth post-EHB star, although it appears to be somewhat too cool and faint to arise from post-EHB tracks.

assigned a random age along the nearest evolutionary track, starting with a ZAHB distribution matched to the observed number and temperature distribution of the HB stars in NGC 6752. In a set of 1000 such simulations, we find a median number of 11 post-EHB stars, and find fewer than five post-EHB stars in only 2.2% of the trials.

The deficit of post-EHB stars in NGC 6752 also appears to persist for the stars for which we do not have optical photometry and hence colors. There are 134 sources on the UIT image outside of the region studied by B86, including 103 sources in the core and 31 sources on the periphery of the cluster. But among these 134 sources, only UIT 1 is sufficiently bright to be a good post-EHB candidate. Note that a deficit of post-EHB stars in the core might be at least partially explained by the deficit of EHB stars reported there by Shara et al. (1995).

If the deficit of post-EHB stars in NGC 6752 is not a statistical anomaly, what changes might be required in the HB models? One possibility would be to decrease the post-EHB lifetime relative to that of the EHB phase. It has sometimes been suggested that this lifetime ratio could be decreased by EHB models that include “breathing pulses” (e.g., Caloi 1989; Renzini & Fusi Pecci 1988), which are sudden increases in the size of the convective core near the end of the HB evolution. Whether or not breathing pulses actually occur, however, remains an open question (Dorman & Rood 1993). Moreover, Sweigart (1994) has found that breathing pulses do not necessarily reduce the post-EHB lifetime below its canonical value.

Alternatively, the deficit of post-EHB stars might be explained by an increase in the critical temperature at which an HB star follows an AGB-manqué track, instead of evolving rapidly back toward the AGB. This explanation is supported by the high effective temperatures of the four post-EHB stars, suggesting that they are descendants of only the hottest ( $\log T_{\text{eff}} > 4.5$ ) HB stars. However, again it is not apparent what changes in the canonical models would produce such a change in the post-HB morphology. One ingredient missing from the canonical models is radiation-driven mass loss, which has been suggested as the cause of the change in surface abundance as stars evolve from helium-poor sdB stars on the EHB to helium-rich sdO stars in the post-EHB phase (MacDonald & Arrieta 1994). However, radiation-driven mass loss would remove additional mass from the envelope and hence would *increase* the number of stars that evolve along AGB-manqué tracks.

We next compare the present results with the helium-mixed models of Sweigart (1996). Figure 4 shows two representative EHB and post-EHB tracks: one for a canonical sequence (*left panel*) and one for a helium-mixed sequence (*right panel*). As discussed below, the helium-mixed sequence is shown using a best-fit distance modulus of  $(m - M)_0 = 13.30$ , rather than the value of  $(m - M)_0 = 13.05$  determined by R96. The canonical sequence in Figure 4 predicts a luminosity gap of  $\sim 0.3$  dex between the end of the HB and the beginning of the post-EHB phase. This gap is a consequence of the interior readjustment that occurs as an HB star exhausts its central helium fuel and begins helium burning in a shell. The surface luminosity during the post-EHB phase gradually increases as the helium shell moves outward in mass, resulting in a rather large predicted luminosity range ( $\sim 0.6$  dex) for the post-EHB stars.

The helium-mixed sequence in Figure 4 has a high envelope helium abundance ( $Y_{\text{env}} \approx 0.5$ ) due to dredge-up of helium

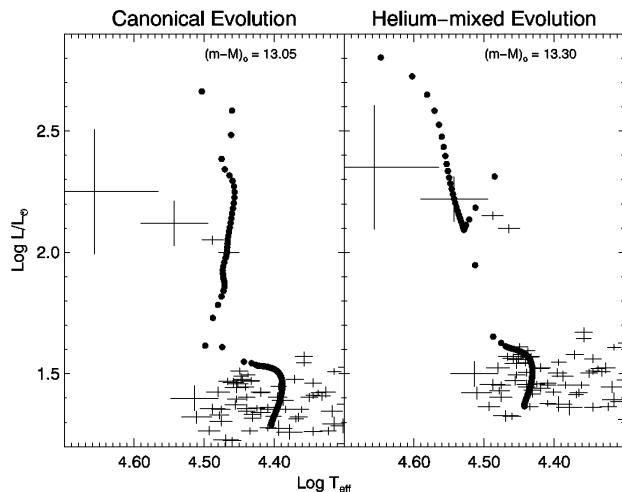


FIG. 4.—Evolution of an EHB star is shown for a canonical HB model (left) and a helium-mixed model of Sweigart (1996) with  $Y_{\text{env}} \approx 0.5$  (right). The rate of evolution is marked every  $5 \times 10^5$  yr. The error bars show the UIT photometry transformed to the theoretical plane assuming  $(m - M)_0 = 13.05$  for comparison with the canonical model, and  $(m - M)_0 = 13.30$  for comparison with the helium-mixed model.

during the preceding RGB phase, and consequently a much larger envelope mass than in canonical models of similar effective temperature ( $\sim 0.03 M_{\odot}$  versus  $\sim 0.006 M_{\odot}$ ). Because of this larger envelope mass, the hydrogen shell reignites at the end of the HB phase. This, together with the increase in the helium-burning luminosity at that time, produces both a larger luminosity gap of  $\sim 0.5$  dex between the HB and the post-EHB phases, and a smaller luminosity range for the post-EHB stars. Figure 4 shows that the four post-EHB stars do cluster near

the luminosities predicted by the helium-mixed track, but the observational and statistical uncertainties are large.

As noted above, the helium-mixed ZAHB is more luminous than the canonical ZAHB, and thus requires a larger distance modulus to fit the NGC 6752 data. However, the ZAHB luminosity of a helium-mixed EHB sequence depends on the mass of its helium core, which, in turn, depends to some extent on the mixing algorithm used along the RGB. The helium-mixed sequence in Figure 4, for example, would be consistent with the R96 distance scale if its core mass of  $0.501 M_{\odot}$  were smaller by  $\sim 0.02 M_{\odot}$ . It is entirely possible that different mixing algorithms might produce such changes in the core mass.

Additional observations could help determine whether the deficit of post-EHB stars in NGC 6752 is a statistical anomaly, and if any modifications are needed to the canonical HB tracks. We have recently obtained a wide-field *UBV* CCD mosaic of NGC 6752 with the goal of improving upon the photographic photometry of B86. In addition, *HST* photometry of the cluster core (e.g., Shara et al. 1995) should allow the CMD to be extended to the entire cluster.

We are pleased to acknowledge the many people involved with the Astro-2 mission who made these observations possible. R. W. O. acknowledges NASA support through grants NAG5-700 and NAGW-4106 to the University of Virginia. A. V. S. acknowledges NASA support through grant NAG5-3028. We thank S. Moehler for showing us her work prior to publication, and B. Dorman and V. Dixon for useful comments. We also thank Yoji Kondo and the staff of the *IUE* observatory for their assistance with the *IUE* observations.

#### REFERENCES

- Bailyn, C. D. 1995, *AR&A*, 33, 133  
 Bohlin, R. C. 1996, *AJ*, 111, 1743  
 Buonanno, R., Caloi, V., Castellani, V., Corsi, C., Fusi Pecci, F., & Gratton, R. 1986, *A&AS*, 66, 79 (B86)  
 Cacciari, C., Fusi Pecci, F., Bragaglia, A., & Buzzoni, A. 1995, *A&A*, 301, 684  
 Caloi, V. 1989, *A&A*, 221, 27  
 Castellani, M., Castellani, V., Pulone, L., & Tornambè, A. 1994, *A&A*, 282, 771  
 D'Cruz, N. L., Dorman, B., Rood, R. T., & O'Connell, R. W. 1996, *ApJ*, 466, 359  
 Dixon, W. V., Davidsen, A. F., Dorman, B., & Ferguson, H. C. 1996, *AJ*, 111, 1936  
 Dorman, B., O'Connell, R. W., & Rood, R. T. 1995, *ApJ*, 442, 105  
 Dorman, B., & Rood, R. T. 1993, *ApJ*, 409, 387  
 Greggio, L., & Renzini, A. 1990, *ApJ*, 364, 35  
 Kurucz, R. L. 1993, *ATLAS9 Stellar Atmosphere Programs and 2 km/s Grid* (Smithsonian Astrophysical Observatory), CD-ROM No. 13  
 Langer, G. E., & Hoffman, R. D. 1995, *PASP*, 107, 1177  
 MacDonald, J., & Arrieta, S. S. 1994, in *Hot Stars in the Halo*, ed. S. Adelman, A. R. Upgren, & C. J. Adelman (New York: Cambridge Univ. Press), 238  
 Moehler, S., Heber, U., & Rupprecht, G. 1996, *A&A*, in press  
 Nichols, J. S., & Linsky, J. L. 1996, *AJ*, 111, 517  
 Peterson, C. J. 1993, in *ASP Conf. Ser. 50, Structure and Dynamics of Globular Clusters*, ed. S. G. Djorgovski & G. Meylan (San Francisco: ASP), 337  
 Renzini, A., & Fusi Pecci, F. 1988, *ARA&A*, 26, 199  
 Renzini, A., et al. 1996, *ApJ*, 465, L23 (R96)  
 Shara, M. M., Drissen, L., Bergeron, L. E., & Paresce, F. 1995, *ApJ*, 441, 617  
 Stecher, T. P., et al. 1992, *ApJ*, 395, 1  
 Stetson, P. B. 1987, *PASP*, 99, 191  
 Sweigart, A. V. 1994, in *Hot Stars in the Halo*, ed. S. Adelman, A. R. Upgren, & C. J. Adelman (New York: Cambridge Univ. Press), 17  
 ———. 1996, *ApJ*, 472, L00  
 Whitney, J. H., et al. 1994, *AJ*, 108, 1350  
 Yi, S., Afshari, E., Demarque, P., & Oemler, A. 1995, *ApJ*, 453, L69